applied sciences

MDPI

Article

Laser Induced Method to Produce Curcuminoid-Silanol Thin Films for Transdermal Patches Using Irradiation of Turmeric Target

Alexandru Cocean [1], Iuliana Cocean [1], Nicanor Cimpoesu [2,*], Georgiana Cocean [3], Ramona Cimpoesu [2], Cristina Postolachi [1], Vasilica Popescu [4] and Silviu Gurlui [1,*]

[1] Faculty of Physics, Atmosphere Optics, Spectroscopy and Laser Laboratory (LOASL), Alexandru Ioan Cuza University of Iasi, 11 Carol I Boulevard, 700506 Iasi, Romania; alexcocean@yahoo.com (A.C.); iuliacocean@gmail.com (I.C.); tina.postolaki@gmail.com (C.P.)

[2] Faculty of Material Science and Engineering, Gheorghe Asachi Technical University of Iasi, 59A Mangeron Boulevard, 700050 Iasi, Romania; ramona.cimpoesu@tuiasi.ro

[3] Rehabilitation Hospital Borsa, 1 Floare de Colt street, 435200 Borsa, Romania; cocean.georgiana@yahoo.com

[4] Department of Chemical Engineering in Textiles and Leather, Gheorghe Asachi Technical University of Iasi, 29 Boulevard Dimitrie Mangeron, 700050 Iasi, Romania; vpopescu65@yahoo.com

* Correspondence: nicanor.cimpoesu@tuiasi.ro (N.C.); sgurlui@uaic.ro (S.G.)

Abstract: A new possible method to produce a transdermal patch is proposed in this paper. The study refers to the pulsed laser deposition method (PLD) applied on turmeric target in order to obtain thin layers. Under high power laser irradiation of 532 nm wavelength, thin films containing curcuminoids were obtained on different substrates such as glass and quartz (laboratory investigation) and hemp fabric (practical application). Compared FTIR, SEM-EDS and LIF analyses proved that the obtained thin film chemical composition is mainly demethoxycurcumin and bisdemethoxycurcumin which is evidence that most of the curcumin from turmeric has been demethixylated during laser ablation. Silanol groups with known role into dermal reconstruction are evidenced in both turmeric target and curcuminoid thin films. UV–VIS reflection spectra show the same characteristics for all the curcuminoid thin films, indicating that the method is reproducible. The method proves to be successful for producing a composite material, namely curcuminoid transdermal patch with silanol groups, using directly turmeric as target in the thin film deposited by pulsed laser technique. Double layered patch curcuminoid – silver was produced under this study, proving compatibility between the two deposited layers. The silver layer added on curcuminoid-silanol layer aimed to increase antiseptic properties to the transdermal patch.

Keywords: PLD; turmeric; curcuminoid-silanol films; transdermal patch; demetoxilation; SEM-EDS; LIF; hemp composite

Citation: Cocean, A.; Cocean, I.; Cimpoesu, N.; Cocean, G.; Cimpoesu, R.; Postolachi, C.; Popescu, V.; Gurlui, S. Laser Induced Method to Produce Curcuminoid-Silanol Thin Films for Transdermal Patches Using Irradiation of Turmeric Target. *Appl. Sci.* **2021**, *11*, 4030. https://doi.org/10.3390/app11094030

Academic Editor: Andrea Li Bassi

Received: 29 March 2021
Accepted: 25 April 2021
Published: 28 April 2021

1. Introduction

Turmeric effects on human's health have been intensively studied lately, after its benefits had been observed during the long time use as spice in food. Extracted from turmeric, curcumin, along with the other curcuminoids, were found as carriers of curative effects for a long list of diseases such as anti-inflammatory including in rheumatoid arthritis, antioxidant, increase of brain-derived neurotrophic factor (BDNF), benefits against depression, [1,2]. Cyto-protective, anticancer properties and immunomodulating effect of turmeric have been also proven [3,4] and its antimicrobial, antioxidant, and astringents properties also recommend it for stomatology and generally, oral uses [5,6]. A turmeric protective effect against natural and chemically-induced toxicity has been also reported [7]. Studies showed favorable piperine influences on pharmacokinetics of curcumin [8];

otherwise, curcumin would not be properly absorbed. However, turmeric itself contains piperine that allows a better absorption into the body, including dermal absorption. Thus, turmeric should be preferred as the basic natural component when to start a new procedure for obtaining derivatives to be used as pharmaceutical products to harness turmeric entirely potential, though the curcumin percentage is said to be low in turmeric. Sometimes, the natural composite components would interact to provide a synergic effect for a highly efficiency in order to obtain the desired purpose.

Hybrid layered double hydroxides-curcumin thin films were obtained through MAPLE (Assisted Pulsed Laser Evaporation) for medical purpose [9] and very encouraging results on the incorporation of curcumin in liquid nano-domains embedded into polymeric films for dermal application were realized [10]. The disadvantage of these methods is that they require the prior extraction of curcumin from turmeric which is difficult and low yield when performed by conventional methods due to the low solubility of curcumin in various solvents [11,12]. The method proposed by this study aims to solve the problem of poor solubility of turmeric in various solvents that makes it less available to pharmaceutical purposes [12].The novelty of the study presented herein consists in use of the technique PLD (Pulsed Laser Deposition) to ablate turmeric and deposit on different materials with the further goal to produce medical devices, mainly as medical transdermal patches. The PLD technique applied directly to the turmeric target is an absolutely new method of extracting curcuminoids from turmeric. The final purpose is to transfer the curcuminoids obtained in the deposited thin layer through skin into the body and/or to heal wounds, dermatitis, to regenerate and prevent infections, silanol groups from turmeric contributing as well to such effects along with the other components. Silanol benefits for the dermal cure have been already proven [13] and have been successfully used in cosmetics.

Double layered patch curcuminoid—silver was also produced under this study and proved compatibility between constituents, with the aim to increase antiseptic properties. Further studies in medical environment of an experimental patch are proposed to several particular clinics and the results will be evaluated in a different article.

2. Materials and Methods

The turmeric powder is of Indian provenience, commercialized in Romania by Sanflora Bucuresti, Romania, with determined humidity of 9.32% and with an average granular size of the order of tens of micrometers, as can be seen from the images obtained by optical microscopy of the turmeric grains compared to a grid of 0.1 mm × 0.1 mm (Figure 1a). From the same optical microscopy images, the tendency of agglomeration and/or aggregation of turmeric powder grains is visible by the presence of particles of different shapes and sizes that reach hundreds of micrometers. However, from the point of view of the procedure used in laser ablation, this is not an impediment, because the powder is to be pressed in order to obtain the target. In this regard, the turmeric powder was pressed using a pressure of 100 atm in a ring-shaped stainless steel mold to form the target. The pressure of 100 atm is enough to compact the powder but should not affect the turmeric properties because when removed from the mold, the resulted powder presents grains of similar size to the bigger grains in the initial turmeric powder, probably due to agglomeration/aggregation during compression (Figure 1b). This means that the physical properties have not undergone any changes or only minor changes, namely related to the aggregation of the grains. Moreover, the pressure was low enough not to induce chemical changes in the compressed turmeric powder. However, the turmeric powder was compressed by the same method, mixed with potassium bromide when the FTIR analysis was performed, the resulting spectra describing exactly the target used for PLD. Images from the preparation of the turmeric powder target by pressing, the positioning of the target in the vacuum chamber, together with images during the pulsed laser deposition process are presented in Figure 2 a–g.

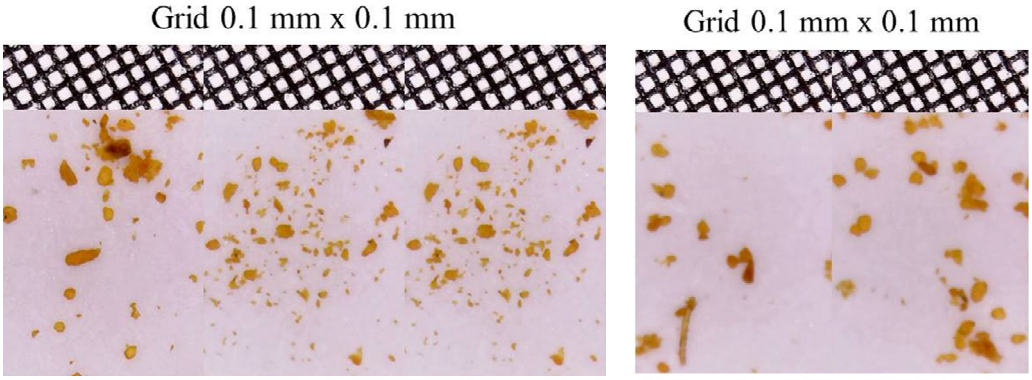

Figure 1. Optical microscope images of Turmeric powder grains compared with a grid scale of 0.1 mm × 0.1 mm before compression in the mold (**a**) and after compression in the mold (**b**).

The resulted target in size of 10 mm radius and 4 mm height was irradiated with 10 ns pulsed laser beam of 336 μm spot radius and 532 nm wavelength with 10 Hz repetition rate, using a YG 981E/IR-10 laser system at 25 J/cm^2 fluence for 30 min, which results in 18,000 pulses [14,15]. Distance between target and support was of 2.5 cm and the pressure in the deposition chamber 10^{-2} Torr. During deposition, the target is moved by a software-assisted mechanism. Due to the circular shape of the target, in this case the spiral movement was selected with the starting point in the center of the target. The equipment used is in Atmosphere Optics, Spectroscopy and Lasers Laboratory (LOASL) and it is presented schematically in Figure 3a. The wavelength of 532 nm is used for turmeric ablation and deposition as it has been previously proven that it preserves the organic structure better with minimum bonds breakage [14].

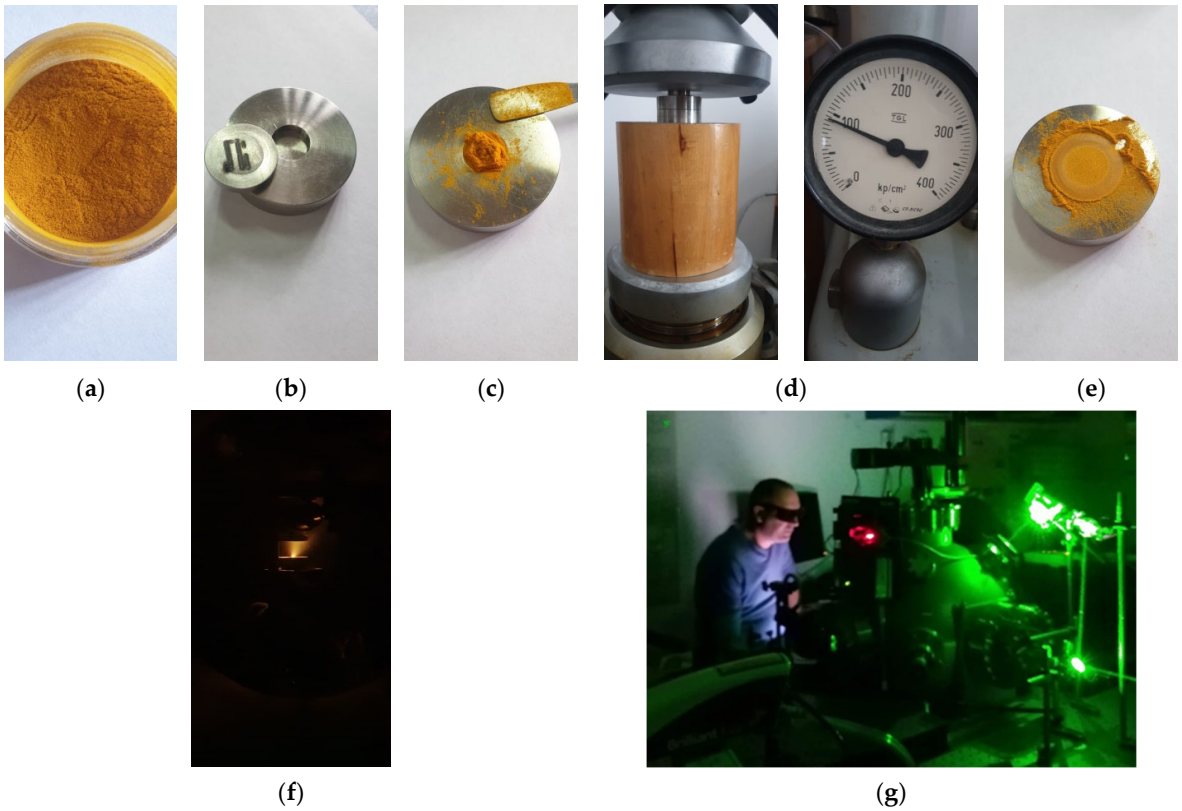

Figure 2. Images of materials and means used to produce the turmeric target and its displacement into the work system: Turmeric powder (**a**), ring-shaped stainless steel mold (**b**), filling the mold with turmeric powder (**c**), pressing the turmeric powder into the mold at 100 atm (**d**), turmeric target formed into the stainless steel ring (**e**), target placed into the vacuum chamber and target irradiation (**f**), images during work with laser beam irradiation at 532 nm wavelength (**g**).

Pulsed laser depositions were performed on glass and quartz slabs (in order to obtain experimental results), as well as on hemp twill fabric (for a possible medical application), Figure 1b. The hemp fabric material was used as substrate in order to observe the practical possibility of growing new thin layers on this type of complex surface. Known antimicrobial and antifungal silver properties, a double layer was also produced aimed to enhance the healing and antiseptic properties. Turmeric was first deposited and then silver thin film on top of it. This way, five samples were obtained: turmeric on glass slab (T/GLS), turmeric on quartz slab (T/QTZ), turmeric on hemp twill fabric (T/HMP), silver on turmeric coating on glass slab (Ag/T/GLS) and silver on turmeric coating on hemp twill fabric (Ag/T/HMP). Images of the material depositions (experimental glass and hemp substrates) were realized using scanning electron microscopy (SEM: VegaTescan LMH II, SE detector, 30 kV) in order to obtain details at higher amplification. Energy dispersive spectroscopy (EDS, Bruker X-flash) was used to identify the chemical elements from the thin layers obtained through PLD.

Fourier transform infrared spectroscopy (FTIR) performed with Versatile FT–IR Laboratory Spectrometer MB3000 on dry powder samples incorporated in potassium bromide provided information on the functional groups of chemical compounds deposited. The information on the chemical composition was completed by LIF spectrometry that was conducted using the UV laser beam of 355 nm wavelength of the same laser system YG 981E/IR-10. For data acquisition, a high resolution spectrometer (750 mm focal length) Acton 2750i coupled with Roper Scientific PIMAX3 ICCD camera, 1024 × 1024 pixels, 2 ns minimum gate time was used.

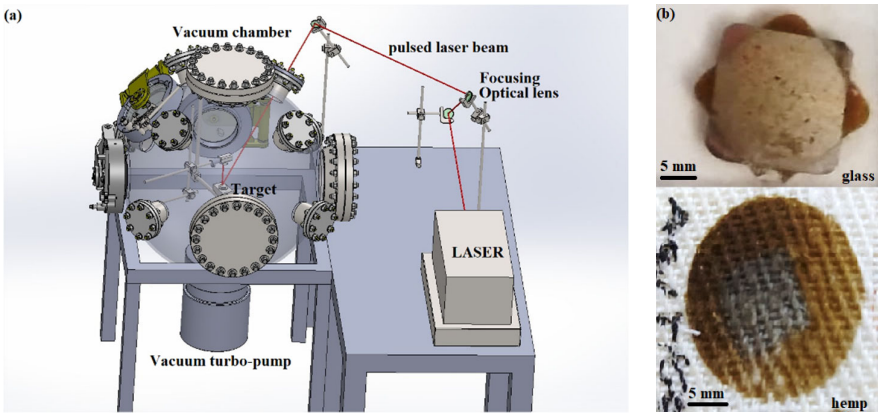

Figure 3. Pulsed laser deposition of Turmeric: (**a**) schematic 3D view of PLD equipment (Atmosphere Optics, Spectroscopy and Lasers Laboratory (LOASL), Faculty of Physics from Alexandru Ioan Cuza University of Iasi); (**b**) depositions of turmeric and silver on glass and hemp fabric.

3. Results

The thickness of the curcuminoid layer produced (Curcuminoid-silanol film/Quartz) measured with Stylus Profiler DektakXT Bruker was found as being of four micrometers on an area of 226.8 mm^2. As this experiment was designed to evaluate quality of deposition and to set-up the parameters and conditions for ablation, the deposition efficiency was not calculated due to the difficulties of accurate measurement of the ablated material on the target. However, given the fine "trace" left on the target by laser radiation due to ablation, compared to the deposition surface and the thickness of the layer, it is expected that the deposition yield with the PLD method will be very high.

A sample of curcuminoid powder was collected scraping the thin film obtained by PLD technique using same procedure as reported before by Cocean et al. [14] and it was used for FTIR analysis, resulting the spectrum of *Curcuminoid-silanol fil***.** FTIR analysis was also performed on turmeric powder used as target, resulting the spectrum of ***Turmeric***, as well as on pure curcumin powder, namely the spectrum of ***Curcumin***. All the three spectra were compared. 5. Curcuminoid-silanol thin films fluorescence was analyzed compared to the turmeric powder using laser induced fluorescence (LIF.. Chemical analysis was completed by elemental composition performed by SEM-EDS spectroscopy when also morphological information was obtained. UV–Vis reflection spectra provided information regarding optical properties of the obtained curcuminoid films ***Curcuminoid-silanol film/Glass***, ***Curcuminoid-silanol film/Quartz***, ***Curcuminoid-silanol film***/HMP, ***Ag/Curcuminoid-silanol film/Glass***, and ***Ag/Curcuminoid-silanol film/Hemp***.

3.1. Fourier Transform Infrared Spectroscopy (FTIR) Analysis

For the deposition with PLD method, the turmeric powder compressed into a disk shape target without any additives was used. That provides information on the starting chemical composition where the specific groups in curcuminoids are expected to be found, such as shown in the chemical formulae in Figure 4. Fourier transform infrared spectroscopy (FTIR) analysis of both target and obtained thin film resulted into spectra of high similitude (Figure 5), proving that curcuminoid-silanol films were obtained.

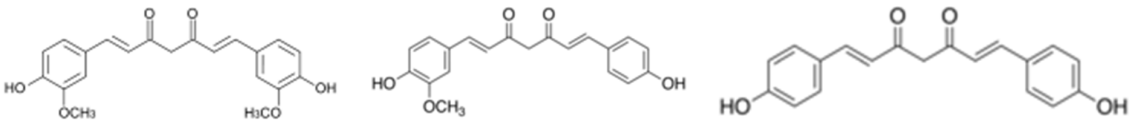

Curcumin Demethoxycurcumin Bisdemethoxycurcumin

Figure 4. Chemical structures of curcuminoids.

In Figure 5, for the ***Turmeric*** FTIR spectrum, predominant curcumin component is observed, while for the thin film obtained by PLD (***Curcuminoid-silanol film*** spectrum), demethoxylation is evidenced by the drastic mitigation in transmittance intensity, which becomes barely visible, of the 2925 cm^{-1} and 2853 cm^{-1} bands specific for C–H aliphatic stretching of the acetal (methoxy) groups O–CH_3, indicating increase in the other two curcuminoid components (demethoxycurcumin, and bisdemethoxycurcumin). Demethoxylation is also denoted by lower intensity of bands in the thin film spectrum compared with the turmeric powder, bands corresponding to specific groups. Therefore, intensity mitigation is noticed for the 1279 cm^{-1} band of the (ar)C–O–(al)C groups stretching asymmetric, usually vibrating in the range (1275–1200 cm^{-1}) [16], in the same range with (ar)C–H in plane deformation vibration (1250–950 cm^{-1}) while the (ar)C–C group expected in the range 3080–3030 cm^{-1} [16] overlaps with the broad peak at 3440 cm^{-1} in turmeric spectrum and it is very weak in the thin film spectrum. Moreover, a decrease of the intensity of the bands is observed for those at 1079 cm^{-1} and 1024 cm^{-1} in the thin film spectrum compared with the turmeric powder spectrum corresponding to (ar)C–O–(al)C stretching symmetric vibrations, usually occurring in the range of 1075–1020 cm^{-1} [16]. In the same range are the specific silanol terminal groups as it is presented below. The other specific vibrations for the curcuminoids are observed in both FTIR spectra of turmeric powder and deposited thin film.

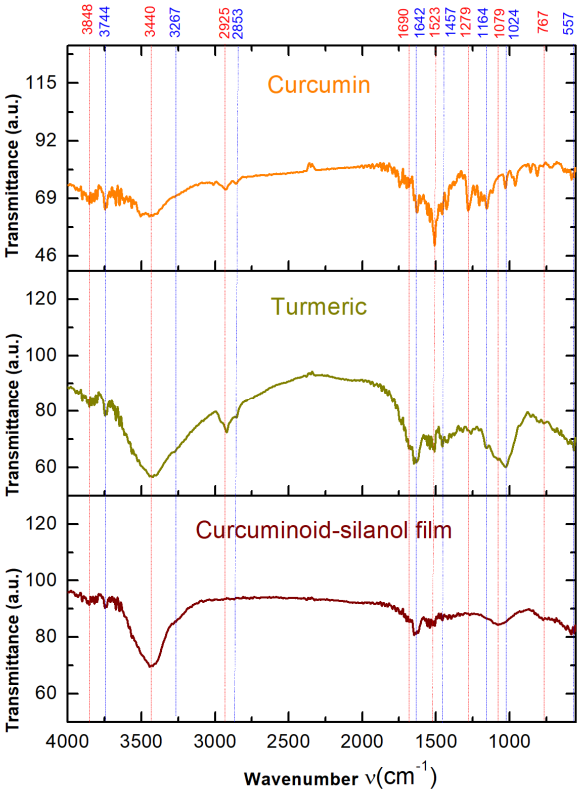

Figure 5. FTIR spectra of curcumin powder (***Curcumin)***, turmeric powder (***Turmeric***), ***Curcuminoid-silanol film*** (thin film obtained by PLD technic)

It is important to notice silanol groups which are identified in both turmeric powder and thin film. Thermal resistivity of the silanol groups explains their preservation during ablation and occurrence in the deposited thin films. The band at 3848 cm^{-1} is of O–H free stretching vibrations [17] that could be associated to Si–OH groups [18] and the 3744 cm^{-1} band has been previously proven and reported for the terminal silanol groups [19–21], the

IR spectroscopy generally assigning the bands in the range 3700–3200 cm^{-1} to Si–OH stretching vibrations [18]. The bands at 1457 cm^{-1} and 1279 cm^{-1} are of the (Si–)CH_3 group asymmetric and symmetric, respectively, deformation vibrations [16]. The 1024 cm^{-1} band of the Si–OH deformation vibrations (~1030 cm^{-1}), but also 1079 cm^{-1} of Si–O–Si stretching vibrations (1090–1030 cm^{-1}) [16] are lower in intensity for the thin film than in the turmeric powder spectrum, showing that some of the silanol terminal groups are removed during ablation process. Silanol terminal groups are also evidenced with the 767 cm^{-1} band assessed to Si–C stretching vibration in the 850–650 cm^{-1} range and to (Si–)CH_3 skeletal vibration that usually occurs at ~765 cm^{-1}) [16].

The O–H free and H-bonded phenolic groups are evidenced by the stretching vibrations at 3440 cm^{-1} [16]. The 3267 cm^{-1} band indicates C–H aromatic stretching vibrations [16], aromatic character being also evidenced in the C=C aromatic skeletal vibrations of 1523 cm^{-1} band [16]. The 2925 cm^{-1} band is assessed to C–H aliphatic stretching [16] together with the C–H stretching vibration in O–CH_3 acetals denoted by the band at 2853 cm^{-1}[14]. The 1690 cm^{-1} band is assessed to C=O stretching, aliphatic, attached to aromatic groups that causes a shift to lower wavenumbers from ~1715 to 1695–1695 cm^{-1} (wavenumber decreases with increasing ring size) [16], a band at 1642 cm^{-1} of C=O stretching vibrations being also present [17]. The band at 557 cm^{-1} indicates C–S groups [16].

3.2. Scanning Electron Microscopy with Energy Dispersive Spectroscopy (SEM-EDS)

SEM analysis provides information on the morphology (Figure 6) and elemental composition (Table 1) of the turmeric powder (*Turmeric*) and the thin films obtained by PLD technic (*Curcuminoid-silanol film)*.

SEM images show polymeric agglomerations for the ***Curcuminoid-silanol film/Glass*** and ***Curcuminoid-silanol film/Hemp*** proving self-organization properties, and a good coating of the fibers in the ***Curcuminoid-silanol film/Hemp***. Added silver particles are uniformly dispersed on top of the curcuminoid thin films and within the hemp fibers from the fabric texture. The dimensions of measured silver particles vary from 2 to 3 μm droplets to a nano-metric layer deposited on the substrate [22]. The second role of silver layer is to fix and sustain the curcuminoid-silanol thin film on the substrate. Both variants with and without very thin silver layer present interests in medical field.

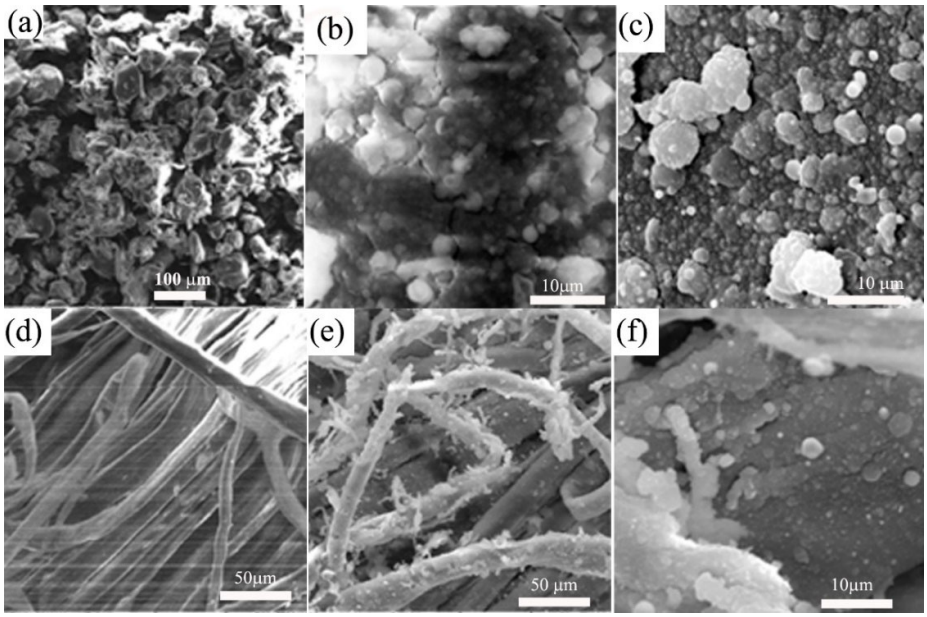

Figure 6. SEM images of turmeric powder (Turmeric) 350× (**a**); Curcuminoid-silanol film/Glass 5kx (**b**); Ag/Curcuminoid-silanol film/Glass 5kx (**c**); Curcuminoid-silanol film/Hemp 1kx (**d**); Ag/Curcuminoid-silanol film/Hemp 1kx (**e**); detail of Ag/Curcuminoid-silanol film/Hemp 5kx (**f**).

Elemental composition shows, among specific organic elements such as carbon and oxygen, an atomic percentage of 0.08% silicon in turmeric powder and 0.04% in the composition of the curcuminoid thin film deposited on hemp. The 0.11% of silicon determined in the ***Curcuminoid-silanol film/Glass*** could be due to the influence of the substrate composition. Carbon elemental composition is similar in turmeric powder and thin films deposited on both glass and hemp, with only slight differences. In atomic percentage, the variation of carbon percentage is from 63.89% in turmeric powder to 65.38% in ***Curcuminoid-silanol film/Glass*** and 65.95% in ***Curcuminoid-silanol film/Hemp***, the latter being under the influence of the hemp substrate composition. The atomic composition of oxygen was of 35.49% for turmeric powder, 29.83% for ***Curcuminoid-silanol film/Glass,*** and 33.43% for ***Curcuminoid-silanol film/Hemp***.

The balance to 100% is split between different other elements such as Fe, Cu, K, Cr, Zn, and they reflect the vegetal material property to absorb metals, the plant roots and rhizomes retaining most of them. The same mechanism made possible absorption of silicon which proves affinity for the curcuminoids to form silanol bond on their terminal groups.

Table 1. Compared elemental composition of turmeric powder and thin films deposited on glass slab and on hemp fabric, respectively.

Element	Atom (%)			Weight (%)			EDS Error %
	Turmeric Powder	Curcuminoid-Silanol Film/Glass	Curcuminoid-Silanol Film/Hemp	Turmeric Powder	Curcuminoid-Silanol Film/Glass	Curcuminoid-Silanol Film/Hemp	
Carbon	63.89	65.39	65.96	56.49	51.84	53.37	2.2
Oxygen	35.49	29.83	33.43	41.80	31.50	39.41	1.2
Iron	0.01	1.62	0.29	0.02	5.96	0.29	0.01
Copper	-	0.99	0.01	-	4.18	0.04	0.09
Potassium	0.53	1.17	0.15	1.52	3.01	0.43	0.11
Chromium	0.01	0.46	0.09	0.01	1.60	0.33	0.1
Nickel		0.31	0.03	-	1.19	0.11	0.13
Zinc		0.12	0.01	-	0.51	0.01	0.05
Silicon	0.08	0.11	0.04	0.17	0.21	0.09	0.05

Standard deviations: C: ±1.2, O: ±0.8, Si: ±0.01, Fe: ±0.001, Cu: ±0.001, K: ±0.001, Cr: ±0.005, Ni: ±0.01 and Zn: ±0.001.

Laser induced fluorescence (LIF). LIF also provides information about chemical structure of the investigated material when fluorophore groups are present and about UV laser beam interaction with the material, which are the curcuminoids in this case. Laser induced fluorescence using 355 nm laser beam wavelength evidenced fluorescence spectra as shown in Figure 7. The sharp peaks at about 514 nm and about 550 nm may be assessed to the sulfur [23] and silanol groups, respectively [24] in the curcuminoid molecules. The latter one was observed for the silanol alkyl groups. Silanol groups have been identified in the FTIR spectra of Figure 5 as terminal groups. That, together with the LIF spectra, shows that some of the silanol groups are bond to the methoxy groups of curcumin, explaining the mitigation in FTIR spectrum intensity of the thin film for both silanol and methoxy. The information from the spectra of Figure 5 is that a partial demethoxylation of curcumin takes place, methoxy groups leaving the molecule together with the silanol groups bond to methoxy. As silanol groups are alkyl ones, their occurrence in the thin film spectrum is an evidence that not all the methoxy groups are removed during ablation and the thin film is a mixture of all the three curcuminoids (curcumin, demethoxycurcumin, and bisdemethoxycurcumin) characteristic to turmeric, just their ratio is changed.

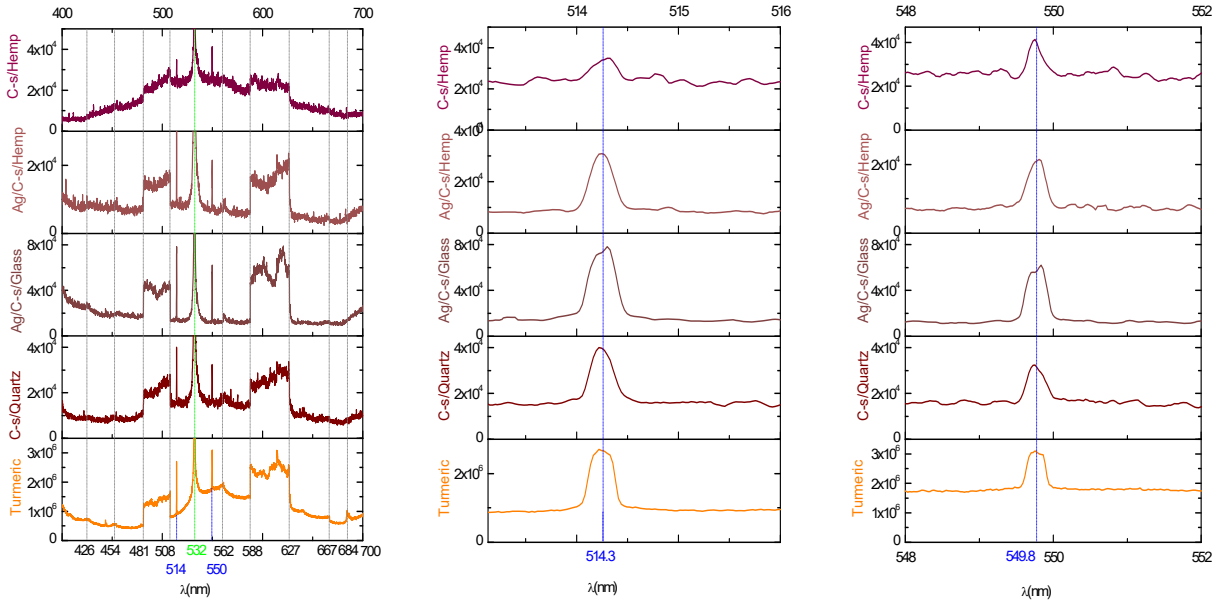

Figure 7. LIF compared spectra of Turmeric, Curcuminoid-silanol film/Quartz (***C-s/Quartz***), and Curcuminoid-silanol film/Hemp (***C-s/Hemp***) and the double layers Ag/Curcuminoid-silanol film/Glass (***Ag/C-s/Glass***) and Ag/Curcuminoid-silanol film/Hemp (***Ag/C-s/Hemp***).

The high ratio of curcumin in the target became low in the thin curcuminoid film, where demethoxycurcumin and bisdemethoxycurcumin predominate.

Specific 562 nm fluorescent emission for turmeric under laser irradiation of 355 nm is lower by two orders (100 times) in intensity for the curcuminoid thin films compared to turmeric powder.

Two tower like structures emissions in 481–508 nm range and 588–627 nm range in all LIF spectra of Figure 7 evidence chemical reactions [25] including radical formation, mainly OH radicals [14]. Secondary peaks are also evidenced at 426 nm, 454 nm, 667 nm, and 684 nm as Swan peaks characteristic to the carbon stars spectra, comets and to burning hydrocarbon fuels [26,27] that here could be from the organic carbon burning during ablation.

Silver thin film deposited on the curcuminoid films produce mitigation in the fluorescent emission due to the shielding effect on the absorption and emission, but also to the interferance with the fluorophore groups of curcuminoids, epecially C = O with high affinity for metals.

3.3. UV–VIS Spectra of Thin Films

In Figure 8, reflection of the 578 nm, 664 nm, and 696 nm light components are noticed. A sharp peak at 436.7 nm is also noticed coming out from the main spectra that could be assessed to the UV lamp irradiation. All the deposited thin films reflect at the same wavelengths and very close intensities (Table 2).

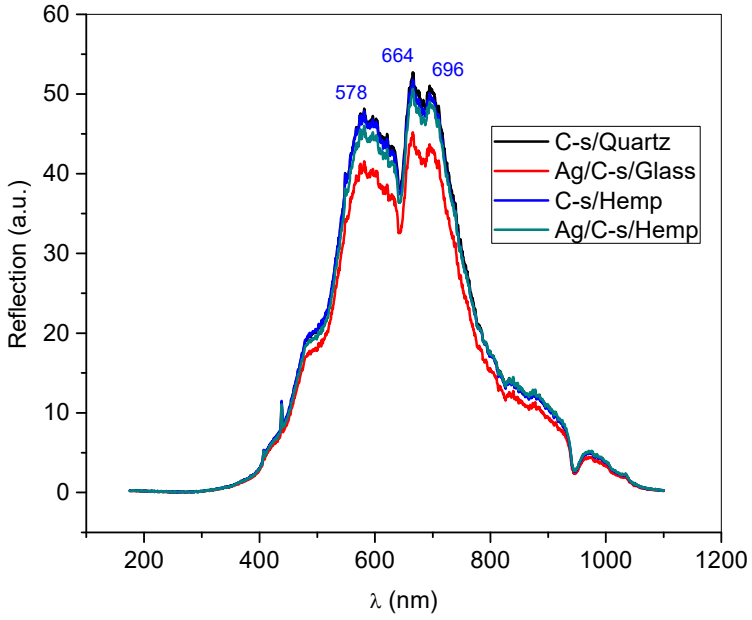

Figure 8. UV–VIS spectra of the thin films reflection properties: Curcuminoid-silanol film/Quartz (***C-s/Quartz***) and Curcuminoid-silanol film/Hemp (***C-s/Hemp***) and the double layers Ag/Curcuminoid-silanol film/Glass (***Ag/C-s/Glass***) and Ag/Curcuminoid-silanol film/Hemp (***Ag/C-s/Hemp***).

The reflection intensity of the curcuminoid layers deposited on hemp decreases only by 0.95% at 578 nm, 0.57% at 664 nm, and 1.75% at 696 nm compared to curcuminoid films deposited on glass. In the case of depositing the additional silver layer, the decrease in intensity of depositions on hemp substrate compared to depositions on glass substrate is 10% at 578 nm, 12% at 664 nm, and 10.8% at 696 nm. In the case of comparison according to the substrate used, there is a decrease of only 4.3% at 578 nm, 2.1% at 664 nm, and 2.78% at 696 nm when the films are deposited on hemp, while when the films are deposited on glass, the differences are 14.83% at 578 nm, 14.4% at 664 nm, and 14.8% at 696 nm. It is observed that the smallest differences are for the single layers of curcuminoids deposited on different substrate (on glass and on hemp), as well as for the double layers of silver and curcuminoids deposited on hemp substrate. The largest variations in reflection intensity are recorded between the deposition of the curcuminoids layer and the deposition of the double layer of silver and curcuminoids on glass substrate. These observations show that the deposition of thin layers of curcuminoids starting from the turmeric target are reproducible with a margin of error below 2%. The increase in the variation of the reflection intensity after the deposition of the second layer, the silver one over the thin layer of curcuminoids, is explained due to the tendency to form droplets. In the case of hemp substrate, the smaller variation than in the case of glass substrate is due to the dispersion of nanoparticles that form the curcuminoid film and the silver and curcuminoid double film among the fibers and microfibrils of the fabric, as seen in electronic microscopy images of Figure 6e,f.

Table 2. Reflection intensities of the thin films deposited.

	Reflection Intensity (a.u.)		
	Λ = 578 nm	Λ = 664 nm	Λ = 696 nm
Curcuminoid-silanol film/Quartz	48.26	52.6	51.2
Curcuminoid-silanol film/Hemp	47.8	52.3	50.3
Ag/Curcuminoid-silanol film/Glass	45.7	51.2	48.9
Ag/Curcuminoid-silanol film/Hemp	41.1	45	43.6

4. Conclusions

New method and new composite materials are reported with this paper. Starting from a natural material, turmeric powder, used as target in the pulsed laser deposition process, the thin films obtained prove to be suitable for medical purposes due to their composition in curcuminoids whose health benefits have been proven. It is also assumed, based on preliminary evaluation, that the method is reproducible which may recommend it for industrial purposes. The method is proven to be a possible solution to the low solubility of turmeric and its components when desired to obtain curcuminoid films or coatings on different substrates. Medical patch for dermal transfer of curative substances containing curcuminoids and silanol can be produced using the method as described herein. Double layered patch curcuminoid – silver is aimed to enhance antiseptic effect of the device. Medical analysis and tests are further required, dosing the quantity of curcuminoid layer deposited needed to provide an optimal transfer over a period of time and for specific diseases.

Author Contributions: Conceptualization, A.C., G.C., C.P., I.C., and S.G.; methodology, I.C., S.G., and A.C.; software, A.C.; validation, A.C., I.C., and S.G.; formal analysis, A.C., C.P., I.C., S.G., N.C., R.C., and V.P.; investigation, A.C., I.C., C.P., G.C., N.C., and S.G.; resources, S.G., N.C. V.P., and I.C.; data curation, A.C., I.C., and S.G.; writing—original draft preparation, I.C., S.G., and A.C.; writing—review and editing, I.C., N.C., R.C., and S.G.; visualization, A.C., S.G., and I.C.; supervision, S.G.; project administration, S.G.; funding acquisition, S.G. and N.C. All authors have read and agreed to the published version of the manuscript.

Funding: This research was funded by Ministry of Research, Innovation and Digitization, project FAIR_09/24.11.2020 and by the Executive Agency for Higher Education, Research, Development, and Innovation, UEFISCDI, ROBIM- project number PN-III-P4-ID-PCE2020-0332.

Institutional Review Board Statement: Not applicable.

Informed Consent Statement: Not applicable.

Conflicts of Interest: The authors declare no conflict of interest.

References

1. Kumar, A.; Singh, A.K.; Kaushik, M.S.; Mishra, S.K.; Raj, P.; Singh, P.K.; Pandey, K.D. Interaction of turmeric (*Curcuma longa* L.) with beneficial microbes: A review. *3 Biotech* **2017**, *7*, 357, doi:10.1007/s13205-017-0971-7.
2. Niranjan, A.; Prakash, D. Chemical constituents and biological activities of turmeric (*Curcuma longa* L.)—A review. *J. Food Sci. Technol.* **2008**, *45*, 109–116.
3. Subtaweesin, C.; Woraharn, W.; Taokaew, S.; Chiaoprakobkij, N.; Sereemaspun, A.; Phisalaphong, M. Characteristics of Curcumin-Loaded Bacterial Cellulose Films and Anticancer Properties against Malignant Melanoma Skin Cancer Cells. *Appl. Sci.* **2018**, *8*, 1188, doi:10.3390/app8071188.
4. Abu-Rizq, H.A.; Mansour, M.H.; Safer, A.M.; Afzal, M. Cyto-protective and immunomodulating effect of *Curcuma longa* in Wistar rats subjected to carbon tetrachloride-induced oxidative stress. *Inflammopharmacology* **2008**, *16*, 87–95, doi:10.1007/s10787-007-1621-1.
5. Alok, A.; Singh, I.D.; Singh, S.; Kishore, M.; Jha, P.C. Curcumin—Pharmacological Actions and its Role in Oral Submucous Fibrosis: A Review. *J. Clin. Diagn. Res.* **2015**, *9*, ZE01–ZE03, doi:10.7860/JCDR/2015/13857.6552.
6. Sood, S.; Nagpal, M. Role of curcumin in systemic and oral health: An overview. *J. Nat. Sci. Biol. Med.* **2013**, *4*, 3–7, doi:10.4103/0976-9668.107253.
7. Hosseini, A.; Hosseinzadeh, H. Antidotal or protective effects of *Curcuma longa* (turmeric) and its active ingredient, curcumin, against natural and chemical toxicities: A review. *Biomed. Pharmacother.* **2018**, *99*, 411–421, doi:10.1016/j.biopha.2018.01.072.

8. Shoba, G.; Joy, D.; Joseph, T.; Majeed, M.; Rajendran, R.; Srinivas, P.S.S.R. Influence of Piperine on the Pharmacokinetics of Curcumin in Animals and Human Volunteers. *Planta Med.* **1998**, *64*, 353–356, doi:10.1055/s-2006-957450.
9. Andrei, F.; Vlad, A.; Birjega, R.; Tozar, T.; Secuc, M.; Urzica, I.; Dinescu, M.; Zavoianu, R. Hybrid layered double hydroxides-curcumin thin films deposited via Matrix Assisted Pulsed Laser Evaporation-MAPLE with photoluminescence properties. *Appl. Surf. Sci.* **2019**, *478*, 754–761.
10. Abramov, E.; Garti, N. Incorporation of curcumin in liquid nanodomains embedded into polymeric films for dermal application. *Colloids Surf. B Biointerfaces* **2021**, *198*, 111468.
11. Carvalho, D.D.M.; Takeuchi, K.P.; Geraldine, R.M.; De Moura, C.J.; Torres, M.C.L. Production, solubility and antioxidant activity of curcumin nanosuspension. *Food Sci. Technol.* **2015**, *35*, 115–119, doi:10.1590/1678-457x.6515.
12. Suresh, K.; Nangia, A. Curcumin: Pharmaceutical solids as a platform to improve solubility and bioavailability. *CrystEngComm* **2018**, *20*, 3277–3296.
13. Herreros, F.O.C.; Cintra, M.L.; Adam, R.L.; De Moraes, A.M.; Metze, K. Remodeling of the human dermis after application of salicylate silanol. *Arch. Dermatol. Res.* **2007**, *299*, 41–45, doi:10.1007/s00403-007-0739-8.
14. Cocean, I.; Cocean, A.; Postolachi, C.; Pohoata, V.; Cimpoesu, N.; Bulai, G.; Iacomi, F.; Gurlui, S. Alpha keratin amino acids BEHVIOR under high FLUENCE laser interaction. Medical applications. *Appl. Surf. Sci.* **2019**, *488*, 418–426, doi:10.1016/j.apsusc.2019.05.207.
15. Cocean, A.; Cocean, I.; Gurlui, S.; Iacomi, F. Study of the pulsed laser deposition phenomena by means of Comsol Multiphysics. *Univ. Politeh. Buchar. Sci. Bull. Ser. A Appl. Math. Phys.* **2017**, *79*, 263–274.
16. Pretsch, E.; Buhlmann, P.; Badertscher, M. Structure Determination of Organic Compounds: Tables of spectral data. *Struct. Determ. Org. Compd.* **2009**, *10*, 978–1007, doi:10.1007/978-3-540-93810-1.
17. Singh, J.; Kaur, N.; Kaur, P.; Kaur, S.; Kaur, J.; Kukkar, P.; Kumar, V.; Kukkar, D.; Rawat, M. Piper betle leaves mediated synthesis of biogenic SnO_2 nanoparticles for photocatalytic degradation of reactive yellow 186 dye under direct sunlight. *Environ. Nanotechnol. Monit. Manag.* **2018**, *10*, 331–338, doi:10.1016/j.enmm.2018.07.001.
18. Blanchard, M.; Méheut, M.; Delon, L.; Poirier, M.; Micoud, P.; Le Roux, C.; Martin, F. Infrared spectroscopic study of the synthetic Mg–Ni talc series. *Phys. Chem. Miner.* **2018**, *45*, 843–854, doi:10.1007/s00269-018-0966-x.
19. Ozkan, S.A.; Ahmed, R. (Eds.) *Novel Developments in Pharmaceutical and Biomedical Analysis*; Bentham Science Publishers: Sharjah, United Arab Emirates 2018.
20. Van Steen, E.; Callanan, L.H. Part 3, Studies in Surface Science and Catalyzes. In *Recent Advances in the Science and Technology of Zeolites and Related Materials, Proceedings of the 14th International Zeolite Conference,* Cape Town, South Africa, *25–30 April 2004*; 2004; Volume 154.
21. Hamdan, H.; Endud, S.; He, H.; Muhid, M.N.M.; Klinowski, J. Alumination of the purely siliceous mesoporous molecular sieve MCM-41 and its hydrothermal conversion into zeolite Na-A. *J. Chem. Soc. Faraday Trans.* **1998**, *24*, 3527–3780.
22. Zakaria, M.A.; Menazea, A.; Mostafa, A.M.; Al-Ashkar, E.A. Ultra-thin silver nanoparticles film prepared via pulsed laser deposition: Synthesis, characterization, and its catalytic activity on reduction of 4-nitrophenol. *Surf. Interfaces* **2020**, *19*, 100438, doi:10.1016/j.surfin.2020.100438.
23. El Sayed, S.; De La Torre, C.; Santos-Figueroa, L.E.; Pérez-Payá, E.; Martínez-Máñez, R.; Sancenón, F.; Costero, A.M.; Parra, M.; Gil, S. A new fluorescent "turn-on" chemodosimeter for the detection of hydrogen sulfide in water and living cells. *RSC Adv.* **2013**, *3*, 25690, doi:10.1039/c3ra45822a.
24. Boom, A.F.J.V.D.; Pujari, S.P.; Bannani, F.; Driss, H.; Zuilhof, H. Fast room-temperature functionalization of silicon nanoparticles using alkyl silanols. *Faraday Discuss.* **2020**, *222*, 82–94, doi:10.1039/c9fd00102f.
25. Tsuboi, Y.; Kimoto, N.; Kabeshita, M.; Itaya, A. Pulsed laser deposition of collagen and keratin. *J. Photochem. Photobiol. A Chem.* **2001**, *145*, 209–214, doi:10.1016/s1010-6030(01)00584-6.
26. Donaldson, L.; Radotic, K.; Kalauzi, A.; Djikanovic, D.; Jeremic, M. Quantification of compression wood severity in tracheids of Pinus radiate D. Don using confocal fluorescence imaging and spectral deconvolution. *J. Struct. Biol.* **2010**, *169*, 106–115, doi:10.1016/j.jsb.2009.09.006.
27. Radotić, K.; Kalauzi, A.; Djikanović, D.; Jeremić, M.; Leblanc, R.M.; Cerovic, Z.G. Component analysis of the fluorescence spectra of a lignin model compound. *J. Photochem. Photobiol. B Biol.* **2006**, *83*, 1–10, doi:10.1016/j.jphotobiol.2005.12.001.